This manuscript was accepted and published by ***Energy & Fuels***, a journal of the American Chemical Society. DOI: 10.1021/ef401118f (http://dx.doi.org/10.1021/ef401118f).
Publication data of the final, corrected work:

Wang, L.; Sandquist, J.; Várhegyi, G.; Matas Güell, B.: CO_2 Gasification of Chars Prepared from Wood and Forest Residue. A Kinetic Study. *Energy Fuels*, **2013**, 27, 6098–6107.

CO_2 Gasification of Chars Prepared from Wood and Forest Residue. A Kinetic Study

Liang Wang,[†] *Judit Sandquist,*[†] *Gábor Várhegyi,*[*,‡] *Berta Matas Güell* [†]

[†] SINTEF Energy Research, PO Box 4761, Sluppen, NO-7465 Trondheim, Norway

[‡] Institute of Materials and Environmental Chemistry, Research Centre for Natural Sciences, Hungarian Academy of Sciences, PO Box 17, Budapest, Hungary 1525

KEYWORDS: Norway spruce, forest residue, biomass, char, kinetics, reactivity, thermogravimetry, CO_2 gasification.

ABSTRACT. The CO_2 gasification of chars prepared from Norway spruce and its forest residue was investigated in a thermogravimetric analyzer (TGA) at slow heating rates. The volatile content of the samples was negligible hence the gasification reaction step could be studied alone, without the disturbance of the devolatilization reactions. Six TGA experiments were carried out for each sample with three different temperature programs in 60 and 100% CO_2. Linear, modulated and constant-reaction rate (CRR) temperature programs were employed to increase the information content available for the modeling. The temperatures at the half of the mass loss were lower in the CRR experiments than in the other experiments by around 120°C. A relatively simple, well known reaction kinetic equation described the experiments. The dependence on the reacted fraction as well as the dependence on the CO_2 concentration were described by power functions (n-order reactions). The evaluations were also carried out by assuming a function of the reacted fraction that can mimic the various random pore / random capillary models. These attempts, however, did not result an in improved fit quality. Nearly identical activation energy values were obtained for the chars made from wood and forest residues (221 and 218 kJ/mol, respectively). Nevertheless, the forest residue char was more reactive; the temperatures at the half of the mass loss showed 20 – 34 °C differences between the two chars at 10°C/min heating rates. The assumption of a common activation energy, *E*, and a common reaction order, *n*, on the CO_2 concentration for the two chars had only negligible effect on the fit quality.

1. INTRODUCTION

Woody biomass has been considered as a main biomass source for bioenergy production, mainly as sawdust, wood chips and cutter shavings. However, the availability of these raw materials is limited and their prices have increased considerably in the last decades.[1] Presently, forest residues, as abundant low-cost biomass resources, are gaining interests and entering the renewable energy market while wood is considered as a raw material for higher-value products. Forest residues are derived from the crown of trees, including usually branches, needles and foliage. Large amounts of forest residues are produced annually. In Norway alone more than 1.5 million m^3 forest residues are harvested and collected annually.[2] Due to the development of collecting and bundling technologies, the recovery and utilization of the forest residues are becoming more important. In contrast to conventional woody biomass, forest residues have more heterogeneous properties in terms of biological components and inorganic elements, which influence their thermochemical conversion.[3]

CO_2 gasification is a promising technology for converting biomass resources into energy and different valuable products.[4] The gasification of the char is an important partial reaction of the biomass-gasification. It is considered to be a rate limiting step because it is kinetically slower than the other partial reactions.[5] Accordingly its kinetics highly impacts the design of the gasifiers.[4]

With the development of biomass carbonization technologies, the CO_2 gasification of biomass charcoal may become a separate technical process in the future. The use of biomass charcoal instead of raw biomass has several advantages in the gasification.[6] Among others, much less tar forms, decreasing the problems caused by the tar deposition in the equipment. The energy efficiency is also higher, compensating partly the energy requirements of the charcoal production.[6] The raw biomass has usually high transport cost and poor grindability, while the chars have higher energy density and improved grindability.[7] Hence the conversion of the forest residues into chars may be a viable possibility to improve the mechanical properties, reduce the logistic costs, and carry out the gasification by simpler and more efficient technologies.

Therefore, it is essential to characterize the CO_2 gasification kinetics of the chars produced from different woody biomass sources. The present work deals with the CO_2 gasification of stem wood and forest residue from Norway spruce [*Picea abies* (L.) Karst], which is a widespread tree species in the Nordic countries. There are several studies on the CO_2 gasification kinetics of woody biomass chars at various operating conditions and char preparation methods.[4,5,8-21] However, none of these studies are dealing with chars prepared from the forest residues of Norway spruce.

The present work aimed at studying the CO_2 gasification process under kinetic control and providing a background for future kinetic sub-models. With its high precision and well-controlled experimental conditions, TGA is a useful tool for studying gasification in the kinetic regime. A major

part of the existing knowledge on the kinetics of the CO_2 gasification of biomass chars is summarized in the extensive review of Di Blasi.[12] If the reaction is far from the equilibrium, then the kinetics usually can be well described by the following type of equations:[12]

$$d\alpha/dt = A_\nu \exp(-E/RT)\, f(\alpha)\, P_{CO_2}^{\nu} \quad (1)$$

where A_ν is the preexponential factor, α is the reacted fraction, function $f(\alpha)$ approximates the reactivity change of the sample as the gasification proceeds, P_{CO_2} is the partial pressure of carbon dioxide, and ν is a formal reaction order. A_ν has a subscript to indicate that the dimension of this quantity varies with ν: if P_{CO_2} is expressed in kPa then the dimension of A_ν is $s^{-1}\,kPa^{-\nu}$. Equations of type 1 are also used for gasification by H_2O or O_2.[22] When the pressure is constant, eq 1 can be rewritten into a more practical form[23]

$$d\alpha/dt = A \exp(-E/RT)\, f(\alpha)\, C_{CO_2}^{\nu} \quad (2)$$

where C_{CO_2} is the dimensionless concentration of CO_2 (v/v) and A has a constant dimension, s^{-1}.

The results reported on the kinetics of CO_2 gasification of biomass chars appear to be rather diverse. For example, the reported activation energies scatter between 82 and 370 kJ/mol.[5,8-15,17-19] Hence particular efforts were made in the present work to obtain dependable kinetic information. This goal was achieved by the following means:

(i) The chars were almost completely devolatilized during the preparation so that the gasification reaction could be studied without the disturbance of a considerable devolatilization;

(ii) The study was based on linear, modulated and constant reaction rate (CRR) experiments so that the obtained kinetics would be valid for very different T(t) programs;

(iii) Care was taken to carry out the experiments in the kinetic regime. The disturbing effects of the transport processes were diminished by low sample masses and slow heating programs.

2. SAMPLES AND METHODS

2.1 Sample Characterization and Preparation. The stem wood and forest residues (containing branches, tops and needles) originated from a Norway spruce forest in East Norway (Hobøl, Latitude 59°43'N and Longtitude 10°52'E) from stands with poor site quality. The Norway spruce trees in this forest are 22-24 m high, with branch sizes between 90 and 180 cm. Their age is above 90 years. Two char samples were prepared from stem wood and forest residues, respectively. The proximate analysis results of raw fuels are presented in Table 1. As shown in Table 1, the total ash of the wood was much lower than that of the forest residue. Table 2 displays the concentration of the ash-forming elements in the raw materials measured by inductively coupled plasma atomic emission spectroscopy (ICP-OES). Table 2 shows that all measured elements had higher concentration in the forest residue. The extent of

this enrichment differed for the different elements, as column 3 indicates. This is a usual behavior, because the plant tissues in the twigs and needles differ from that of the stem wood.[24] The received samples were first milled in a cutting mill equipped with 1 mm bottom sieve, then dried for 24 h at 105 °C in a drying oven. Afterwards the chars were prepared at 950°C following the carbonization procedure of ASTM standard E872-82, which serves to determine the amount of volatile matter in particulate wood fuels. In this way the chars used in the study could be regarded as the "fixed carbon" of the raw materials and the standard volatile content of the samples was zero by definition. Obviously some devolatilization may occur above 950°C but we did not observe considerable TGA signal in the domain of the kinetic evaluation (650-1000°C) during a heating in inert gas flow. The total ash of the chars was 2 and 12%, respectively, as calculated from the data Table 1.

Table 1: Proximate Analysis of Raw Materials Used for Char Preparation[a]

	Wood	Forest residue
Volatile matter	86.1	77.8
Fixed carbon	13.6	19.6
Ash	0.3	2.6

[a] % (m/m), dry basis, by ASTM standard E 871 and D 1102.

Table 2. The Concentration of Ash Forming Elements in the Raw Materials[a]

	Forest residue	Wood	Ratio[b]
Ca	6479	719	9.0
Si	3399	456	7.5
K	2747	584	4.7
Na	31	7	4.4
Mg	408	169	2.4
Al	140	9	15.6
P	402	28	14.4
S	248	42	5.9
Ti	9	1	n.a.
Cr	2	1	n.a.
Mn	409	145	2.8
Fe	67	16	4.1
Cu	3	1	n.a.
Zn	49	10	4.9
Ba	25	10	2.5

[a] ppm (mg/kg, dry basis). [b] Ratio of the concentrations of the forest residue and the wood. (It is not given for the concentrations near to the sensitivity of the equipment.)

The particle size distribution of the obtained chars was measured by laser diffractometer (Beckman Coulter LS230 Laser Diffraction Particle Size Analyzer). The mean particle size of the chars from wood and forest residues was 69 and 75 µm, respectively. 90% (v/v) of the particles were above 16 and 18 µm in the two chars, respectively. Less than 1% (v/v) of the chars were below 4 µm. The Brunauer-Emmett-Teller (BET) specific surface areas were 271 and 205 m^2/g for charcoal produced from the stem wood and forest residues, respectively. These values were measured by BET analyzer Micromeritics Tri Star 3000 at -195.8 °C with N_2 as adsorbate after a degasing of 48 hours at room temperature.

2.2 Experimental Setup and Procedure. The reactivity studies were conducted in a Q5000 IR analyzer from TA instruments which has a sensitivity of 0.1 µg. 60% v/v CO_2-argon mixture and pure CO_2 were used as purge gas with a gas flow of 25 mL/min. The reason for using argon in the ambient gas was connected to its atomic mass (40), which is close to that of CO_2 (44). In this way, its diffusion properties are also close to those of CO_2. Particular care was taken to avoid the presence

of oxygen traces because a char + O_2 reaction would result in disturbing TGA signals. The initial sample mass was around 1 mg to avoid the self-cooling of the samples that the high endothermic reaction heat may cause. For a comparison, another set of experiments were carried out at ca. 2 mg initial sample masses. At this sample mass, however, the transport processes influenced the DTG curves as shown in Section 3.1. The sensitivity and stability of the equipment did not allow to use initial sample masses below 1 mg at the given experimental conditions. Note that the use of low initial sample masses is not unusual in biomass research by TGA. Among other, Khalil et al. employed 1 mg initial sample masses in a char gasification work,[14] while Várhegyi et al. used 0.2 – 0.6 mg initial sample masses in a TGA work on char combustion kinetics.[23]

We did not employ isothermal kinetics because the concept "isothermal" involves a substantial transient time which is lost from the evaluation of the thermogravimetric experiments. If the reacting gas is introduced after reaching the desired isothermal temperature, the transient time is connected to the complete flush out of the inert gas from the apparatus. On the other hand, if the reacting gas is introduced prior to the heating then the reaction during the heat-up is lost from the evaluation.

Three temperature programs were used:

(i) linear T(t) with a heating rate of 10°C/min;

(ii) modulated T(t), where sinus waves with 5°C amplitudes and 200 s wavelength were superposed on a 10°C/min linear T(t);

(iii) "constant reaction rate" (CRR) T(t), when the employed equipment regulated the heating of the samples so that the reaction rate would oscillate around a preset limit.[25] The limit was set to $-dm/dt \approx 10^{-4}\ s^{-1}$, where m is the sample mass normalized by the initial sample mass. This is equivalent to a limit of around 0.1 µg/s at the employed initial sample mass. The T(t) program for such an experiment depends on the behavior of the given sample under the given experimental conditions. As the figures in Section 3.4 indicate, the gasification took place at much lower temperatures in the CRR experiments than in the experiments with linear and modulated T(t). (See Section 3.5, too.)

The modulated and CRR temperature programs were employed to increase the information content of the data, as outlined in earlier work.[26,27] From one point of view, the linear T(t) experiments are rather similar to each other, hence their information content is limited.[28] From another point of view, an acceptable kinetic model should describe well the experiments at any T(t), including the highly irregular CRR temperature programs, too.[26,27]

The above experimental setup resulted in 12 experiments (two samples, two CO2 concentrations and 3 temperature programs). The temperature programs included an extremely slow heat-up (at the CRR experiments) and a moderate heating rate (at the linear and the modulated experiments). Higher heating rates were not employed because we wanted exclude the possibilities of a heat transfer control in the present study.

2.3. Numerical Methods. Fortran 95 and C++programs were employed for the numerical calculations and for graphics handling, respectively. The employed numerical methods have been described in details earlier.[29] The kinetic evaluation was based on the least squares evaluation of the -dm/dt curves. The method used for the determination of -dm/dt does not introduce considerable systematic errors into the least squares kinetic evaluation of experimental results.[30] The model was solved numerically along the empirical temperature – time functions. The model parameters were determined by nonlinear least squares minimization, as outlined in the next section.

2.4. Evaluation by the Method of Least Squares and Characterization of the Fit Quality.

The kinetic evaluation was carried out by the method of least squares. Such values are searched for the unknown model parameters that minimize the following objective function:

$$of = \sum_{k=1}^{N_{exper}} \sum_{i=1}^{N_k} \frac{\left[\left(\frac{dm}{dt}\right)_k^{obs}(t_i) - \left(\frac{dm}{dt}\right)_k^{calc}(t_i)\right]^2}{N_k h_k^2} \quad (3)$$

Here N_{exper} is the number of experiments evaluated together; its value in the present work was 12. N_k denotes the number of t_i time points on a given curve and m is the sample mass normalized by the initial sample mass. The division by h_k^2 serves for normalization, as explained below. Usually h_k is the highest observed value of the given experiment. The normalization by the highest observed values in the least squares sum assumes implicitly that the relative precision is roughly the same for all experiments. This assumption has proved to be useful in numerous works on non-isothermal kinetics since 1993.[31] Among others, two antecedents of the present work also used it.[14,26] However, the magnitude differences were very high in the present work. The peak maxima of the CRR experiments scattered around a very low value, 9×10^{-5} s^{-1}, while the peak maxima of the 10°C/min and modulated experiments were around 18 and 19 times higher, respectively. The ratio of the highest and lowest peak maxima was 27 in the given set of the experiments. Test calculations showed that one cannot assume approximately equal relative precisions at such high magnitude differences. No information was available on the absolute and relative precision of the *-dm/dt* values in the CRR experiments, hence the choice of the h_k of the CRR experiments could not be based on theoretical considerations. Following a recent work,[27] an arbitrary $h_k=5\times10^{-4}$ s^{-1} value was used for the CRR experiments which is ca. 5 times higher than their peak maxima. Accordingly h_k in eq 3 is defined as

$$h_k = \max[\, 5 \times 10^{-4}\,,\ max\left(-\frac{dm}{dt}\right)_k^{obs}\,] \quad (4)$$

The fit qualities obtained in this way are shown in Sections 3.3-3.4. The obtained fit quality can be characterized separately for each of the experiments evaluated together. The deviation between the observed and calculated DTG values of a given experiment is given as a root mean square (rms):

$$dev_k\,(\mu g/s) = \left\{ N_k^{-1} \sum_{i=1}^{N_k} \left[\left(\frac{dG}{dt}\right)_k^{obs}(t_i) - \left(\frac{dG}{dt}\right)_k^{calc}(t_i) \right]^2 \right\}^{½} \quad (5)$$

Here subscript *k* indicates the experiment in the series evaluated and *G* is the TGA signal in unit µg without normalization.

The deviations defined by eq 5 can also be expressed as percent of the corresponding peak maximum:

$$rel.dev_k\,(\%) = 100\; dev_k \,/\, \max\left(\frac{dG}{dt}\right)_k^{obs} \quad (6a)$$

The same relative deviations can obviously be calculated from $-dm^{obs}/dt$ values, too, because the *G* and *m* values differ only by a constant divisor:

$$rel.dev_k\,(\%) = 100 \left\{ N_k^{-1} \sum_{i=1}^{N_k} \left[\left(\frac{dm}{dt}\right)_k^{obs}(t_i) - \left(\frac{dm}{dt}\right)_k^{calc}(t_i) \right]^2 \right\}^{1/2} \Big/ \max\left(\frac{dm}{dt}\right)_k^{obs} \quad (6b)$$

In the tables of the present work the magnitude of the objective function will be characterized by $100\sqrt{of}$ because this quantity is related to the relative deviations by eq 6b.[27] If all h_k were equal to the corresponding peak maxima, $100\sqrt{of}$ would be equal to the root mean square formed from the relative deviations of the evaluated experiments.

3. RESULTS AND DISCUSSION

3.1. Effect of the Initial Sample Mass and CO_2 Concentration. Figures 1a and 1b compares the behavior of the wood and forest residues samples, respectively, at 10°C/min heating rate, in 60% and 100% CO_2, at 1 and 2 mg initial sample masses. This comparison indicates that the char prepared from forest residue reacts at lower temperatures than the wood char. The temperatures were read at the half of the mass loss as a simple, comparable characteristic. These values showed 20 – 34 °C differences between the two chars at 10°C/min heating rates. The observed behavior can be attributed to the catalytic effect of the high ash content of the forest residue. Note that the majority of the cations listed in Table 2 have proved to have catalytic activities on the char gasification.[8,19]

The samples with 2 mg initial mass (colors magenta and green) reacted at higher apparent temperatures than their counterparts with 1 mg initial sample mass (colors dark red and dark blue, respectively). This behavior indicates a self-cooling effect at the higher sample mass: the real temperature in the sample was lower than the one measured by the equipment. It is worth noting that this effect was particularly visible in the case of the wood char sample, which gasified at higher

temperatures with higher reaction rates. In the following treatment the results obtained from the 1 mg experiments are detailed because they are less influenced by the heat transfer problems.

The CO_2 concentration had a particularly significant effect on the curves, as it can be expected from the literature.[12] As mentioned above, this effect is expressed by factor $C_{CO_2}^{\nu}$ in eq 2.

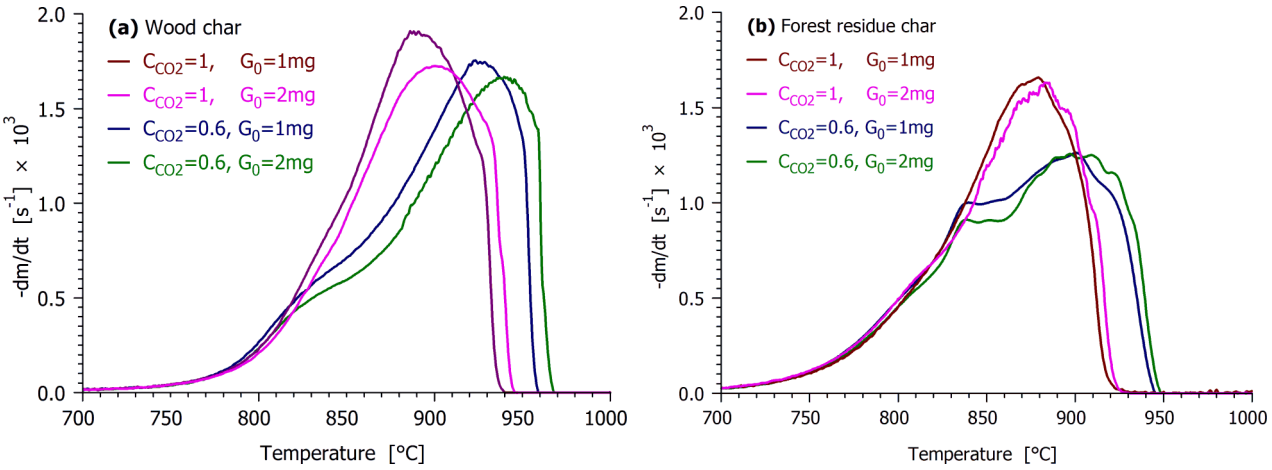

Figure 1. Effect of the initial sample mass and the CO_2 concentration on the char gasification rates with 10°C/min heating rate.

3.2. The Employed Model. Eq 2 in the Introduction shows the family of models considered. Eq 2 describes the change of the reacted fraction during any T(t). α has the following connection with m^{calc}:

$$\alpha(t) = \frac{1-m^{calc}(t)}{1-m_{\infty}^{calc}} \qquad (7)$$

Here m_{∞}^{calc} is the ash yield predicted by the model (i.e. m^{calc} at t=∞). The numerical solution of eq 2 at the T(t) functions of the experiments provides the $\alpha(t)$ functions which belong to the given set of parameters. $m^{calc}(t)$ is calculated from $\alpha(t)$ by eq 7 and is used to get the objective function of the least squares minimization by eq 3.

In one part of the evaluations m_{∞}^{calc} was regarded as an unknown parameter and was determined together with the other model parameters with the constraint of $m_{\infty}^{calc}\geq 0$. This approach resulted in m_{∞}^{calc}=0 for the wood char and in values between 0.11 and 0.13 for the forest residue char. However, the model is not sensitive for the fine adjustment of the values of this parameter. Hence m_{∞}^{calc} was set to its proximate analysis values: m_{∞}^{calc}=0.02 for the wood char and m_{∞}^{calc}=0.12 for the forest residue char. The fit quality only negligibly changed in this way. All the model variants of this work were evaluated with and without the fixing of m_{∞}^{calc} and the results were practically the same.

An essential question is the type of $f(\alpha)$ in eq 2. If the internal pores take an important role in the reaction, a self-accelerating kinetics can be expected. There are theoretical models for that situation in the literature that have been deduced for ideal cases with pure carbon particles of regular shape.[32,33] The gasification of a real char, however, can be altered from the ideal behavior by several complicating factors, including the presence of the mineral matter and the irregular geometry. Hence a simple empirical formula can be used instead of a theoretical one that can mimic a wide varieties of shapes[34]

$$f(\alpha) \cong normfactor\ (1-\alpha)^n\ (\alpha+z)^a \tag{8}$$

where $n>0$, $a\geq 0$ and $z>0$ are adjustable model parameters that define the shape of $f(\alpha)$ and *normfactor* ensures that max $f=1$.

When a=0, eq 8 reduces to n-order kinetics with respect to the reacted fraction:

$$\frac{d\alpha}{dt} = A\ C_{CO_2}^{\nu} \exp(-\frac{E}{RT})\ (1-\alpha)^n \tag{9}$$

The evaluation by equations 8 and 9 resulted in similar fit qualities and parameters. Accordingly the simpler eq 9 was used in the model with unknown parameters of A, E, ν, and n.

3.3. Evaluation by Assuming Common Parameters. If part of the model parameters is assumed to be common for all samples, two benefits can be achieved:

(i) The common parameters indicate the similarities in the kinetic behavior of the samples;

(ii) A given parameter value is based on more experimental information; hence it is less dependent on the various experimental uncertainties.

Table 3 shows a selection of the assumptions employed. The basic case is Evaluation 1 where none of the parameters was assumed to be common. Here the term Evaluation means the application of the method of least squares to the 12 experiments, as described in Section 2.4. The identifier after the word Evaluation refers to a given set of assumptions on the parameters. All parameters, including the parameters common for both samples, were determined by the method of least squares. Evaluation 1 resulted in similar values of E for the wood and forest residue chars: 221 and 218 kJ/mol, respectively. Accordingly a common E for the two chars could be assumed without a loss in the fit quality. (See Evaluation 2 in Table 3.) In this way the number of parameters obtained by the least squares minimization changed to 7: one E value and two values of A, ν, and n were determined.

The difference between the corresponding ν values were more substantial (0.93 and 0.82), nevertheless the assumption of a common ν for the two chars has only a slight effect on the fit quality, as the comparison of the $100\sqrt{of}$ values of Evaluations 3 and 1 indicate in Table 3. This observation supports the similar result of Khalil et al., who also assumed common E and ν values for different chars.[14] Accordingly this model is not sensitive to smaller alterations of ν.

The *n* values also showed some differences (they were 0.45 and 0.57 in Evaluation 1), though the shapes of the corresponding f(α) functions were similar, as shown in Figure 2. Nevertheless, the assumption of common *n* values resulted in a higher increase of the objective function, as the $100\sqrt{of}$ values of Evaluations 4 and 5 indicate in Table 3. However, the increase of $100\sqrt{of}$ from Evaluation 1 (4.80) to Evaluation 5 (5.23) is not high; hence Evaluation 5 is also a viable approximation.

Table 3: Evaluations with various groups of common model parameters

Evaluation	Common parameters	N_{param}	$\frac{N_{exper}}{N_{param}}$	$100\sqrt{of}$
1	none	8	1.5	4.80[a]
2	*E*	7	1.7	4.80
3	*E*, *ν*	6	2	4.83
4	*E*, *n*,	6	2	5.21
5	*E*, *ν*, *n*	5	2.4	5.23

[a] Though the experiments were evaluated in two groups in Evaluation 1, a $100\sqrt{of}$ value for all the 12 experiments is presented here, so that it can be compared directly with the other values in this column

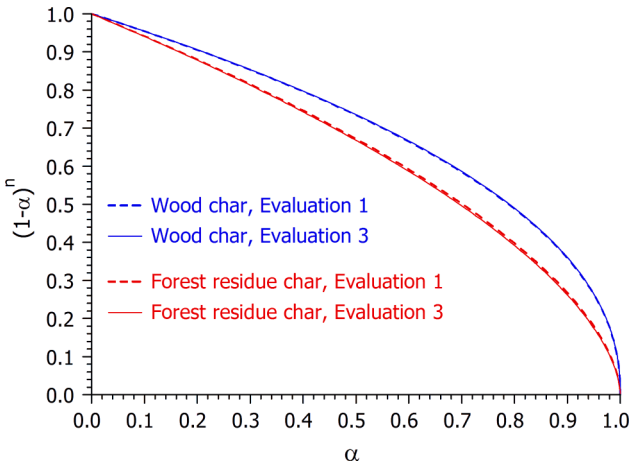

Figure 2. The shape of the $f(\alpha)=(1-\alpha)^n$ functions in Evaluation 1 (dashed lines) and 3 (solid lines). (α is the reacted fraction of the char. α=1 denotes the hypothetic point were only ash remains from the sample.)

In the next section the results of Evaluation 3 will be shown in details. Nevertheless, we believe that Evaluation 5 is also an interesting alternative. At a given T(t) function the width and shape of the calculated curves depend almost entirely on *E* and *n*, while parameter *A* can shift the curve up or down on the temperature axis. Hence the difference between the chars is expressed by a shift on the temperature axis in Evaluation 5.

3.4. Results of Evaluations 3. The fit quality obtained in Evaluation 3 is shown in Figure 3, where the observed and calculated curves are denoted by colors gray and red, respectively. The experimental T(t) functions are displayed by green dashed lines in the plots of the modulated and CRR experiments in Figure 3. The deviation and the relative deviation values, as defined by equations 5 and 6, are also indicated. The difference between the experimental and simulated curves appears to be high in the figures of the CRR experiments. However, the height of these curves is very low; hence the high relative deviations correspond to low deviations. The rms relative deviation of the CRR experiments is 16.8% while the rms deviation of the CRR experiments is 0.016 µg/s. Based on our earlier experience with CRR experiments of similarly low mass loss rates,[27] we believe that the observed low deviations, 0.01 – 0.02 µg/s, are not far from the experimental uncertainties of the CRR experiments. Note that the rms deviation of the experiments with linear and modulated T(t) is ca. 6 times higher, 0.094 µg/s, while their relative deviations is between 3 and 9%. These latter values mark an approximation with a reasonable precision, keeping in mind the relatively simple model, the low number of the adjustable parameters, and the high number of the experiments described simultaneously.

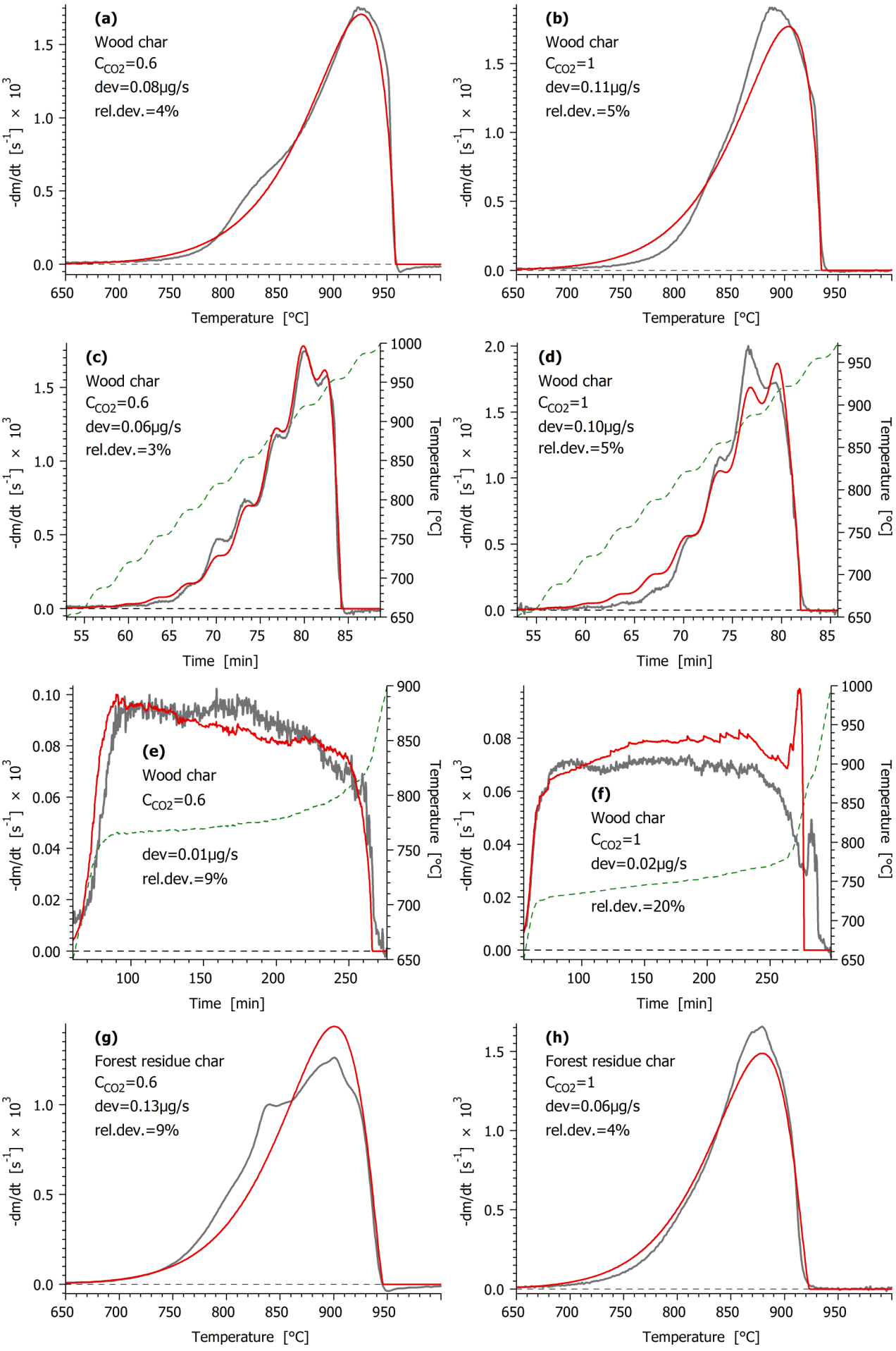
(a)
Wood char
C_{CO2}=0.6
dev=0.08µg/s
rel.dev.=4%
(b)
Wood char
C_{CO2}=1
dev=0.11µg/s
rel.dev.=5%
(c)
Wood char
C_{CO2}=0.6
dev=0.06µg/s
rel.dev.=3%
(d)
Wood char
C_{CO2}=1
dev=0.10µg/s
rel.dev.=5%
(e)
Wood char
C_{CO2}=0.6
dev=0.01µg/s
rel.dev.=9%
(f)
Wood char
C_{CO2}=1
dev=0.02µg/s
rel.dev.=20%
(g)
Forest residue char
C_{CO2}=0.6
dev=0.13µg/s
rel.dev.=9%
(h)
Forest residue char
C_{CO2}=1
dev=0.06µg/s
rel.dev.=4%
-dm/dt [s^{-1}] × 10^3
Temperature [°C]
Time [min]

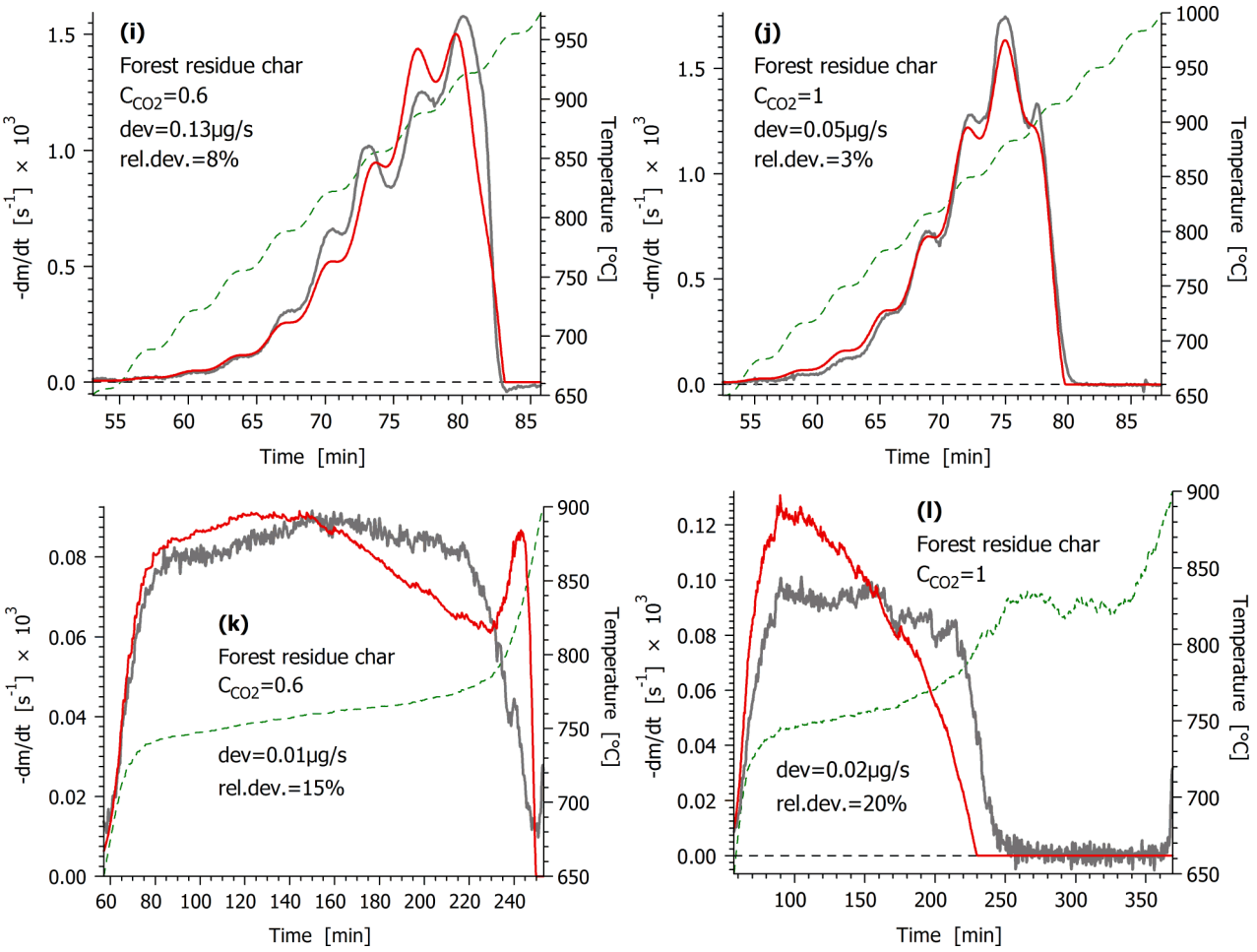

Figure 3. Evaluation of the 12 experiments assuming common *E* and ν values (Evaluation 3 in Table 3). Notation: experimental DTG curves normalized by the initial sample mass (gray —); their calculated counterpart (red —); modulated and CRR temperature programs (green - - -).

The obtained parameters are shown in Table 4. As mentioned in Section 2.2, a set of parallel experiments was measured with around 2 mg initial sample masses. In that case the experiments with linear and modulated heating programs evidenced measurable thermal lags that can be due to heat transfer problems. (See Section 3.1 and Figure 1.) Accordingly, the simultaneous evaluation of these experiments together with the very slow CRR experiments could be done only with a worse fit quality than in the series of the 1 mg experiments. Nevertheless, the resulting parameters were similar, as Table 4 reveals. The difference between the corresponding *E* values is only 4.7 kJ/mol. Note that the activation energy of a simple first order reaction showed higher scatterings in a round-robin study on TGA kinetics.[35] The preexponential factors follow mainly the corresponding activation energy values due to the well-known compensation effect between *E* and *A*. The *n* values are nearly identical in the two cases while the *ν* values show some differences. Alltogether these values in Table 4 indicate that the heat transfer problems of the 2 mg experiments had little effect on the resulting parameters.

The comparison of the present results to earlier works is difficult due to the differences in the experimental conditions, models, and evaluation methods. The closest match to the present study is the work of Khalil et al.[14] Khalil et al. also used 1 mg sample mass to avoid the heat transfer problems and the kinetic evaluation was based on several experiments with different T(t) by the method of least squares. Those kinetic parameter values were selected from that work into Table 4 that were obtained by assumptions identical to Evaluation 3 of the present work. The activation energy of Khalil et al. was higher (265 kJ/mol) and ν was lower (0.40) than the corresponding values of the present work. The *n* values were similar while the higher preexponential factors were a consequence of the higher *E* values, as mentioned above. The causes of the listed differences are not known; probably further investigations are needed in the field. There is an important difference between the two works, however: Khalil et al. studied the simultaneous occurrence of devolatilization and gasification reactions and resolved these processes approximately by the reaction kinetic model itself. On the other hand, the present work used devolatilized chars. The higher ν values of the present work can be regarded more realistic in the kinetic control because one can expect a nearly linear dependence on the CO_2 concentration in the employed domain of experimental conditions. The lower ν values of Khalil et al. may be attributed to the role of devolatilization in the gasification because the devolatilization stage of the reaction is not supposed to depend considerably on the CO_2 concentration.

Table 4: Parameters obtained by Evaluation 3 from Two Series of 12 Experiments with Results from an Earlier Work for Comparison[a]

	Experiments with 1 mg initial sample mass		Experiments with 2 mg initial sample mass		Results from an earlier work[14]	
	Wood char	Forest residue char	Wood char	Forest residue char	Birch char	Pine char
E / kJ mol^{-1}	221	=	225	=	262	=
ν	0.89	=	0.81	=	0.40	=
n	0.44	0.58	0.45	0.58	0.44	0.75
$\log_{10} A$/s^{-1}	7.32	7.54	7.47	7.70	9.02	9.25

[a] "=" indicates parameter values that were assumed to be identical for both evaluated chars.

3.5. Tests on the Difference between the Gasification at Highly Different Reaction Rates and Reaction Temperatures. As mentioned above, the gasification rate in the CRR experiments were much lower than in the experiments with linear and modulated *T(t)*. The average difference was around 18-19 times. The reaction temperatures were also much lower in the CRR experiments. The

evaluation software determined and listed the temperatures of a few characteristic points on the calculated $\alpha(t)$ curves, including the temperatures belonging to α=0.5. These temperatures, denoted here by $T_{0.5}$, were around 120°C lower in the CRR experiments than in the rest of the experiments. (The difference between the arithmetic means of these values, $\overline{T_{0.5,lin\&mod}} - \overline{T_{0.5,CRR}}$ was 121 – 122°C in all evaluations listed in Table 3.) The question arises: is the kinetics truly the same at so different experimental conditions? Test evaluations were carried out to clarify these aspects. Their results are summarized in Table 5. The basis of the tests was Evaluation 3. Parts of the kinetic parameters were allowed to be different for the CRR experiments so that a potential difference between the CRR and the other experiments could be manifested in the changes of the corresponding parameters. Everything else was the same as in Evaluation 3.

In the first test A was allowed to have different values for the CRR experiments: there were separate A_{CRR} and $A_{lin\&mod}$ parameters for the CRR experiments and for the experiments with linear and modulated T(t), respectively. Hence the number of A parameters increased from 2 to 4 and the number of adjustable model parameters, N_{param} increased from 6 to 8. Note that an increase of A shifts the corresponding simulated curve to lower temperatures. If there was a systematic difference in the temperature measurements of the CRR and the other experiments, the changes of the A parameters could have compensated to a certain extent and a better fit quality would have been observed. Among others, calibration problems can be detected in that way. Similarly, if the reactivity of the samples would be different in the experiments measured at lower and higher temperatures, it would result in considerable differences between A_{CRR} and $A_{lin\&mod}$. However, the fit quality practically remained the same: the value of $100\sqrt{of}$ decreased only from 4.83 to 4.82 in Test Evaluation i and the differences between A_{CRR} and $A_{lin\&mod}$ proved to be negligible. In Test Evaluations ii – iv a second parameter was also allowed to be different for the CRR experiments. In this way the system has more possibilities to describe the reactivity differences, if any, caused by the ca. 120°C temperature differences. Here E can affect the width of the calculated curves; ν influences the difference between the experiments at C_{CO_2}=0.6 and 1, as shown by eq 2, while a change of n alters the shape of the $f(\alpha)$ function. In Test Evaluations v and vi, three parameters were allowed to be different for the CRR experiments. None of the test evaluations resulted in a considerable improvement of the fit quality. The change of the kinetic parameters also remained small or moderate, as Table 5 indicates. The largest changes were observed in test evaluation vi. Here the question arises: how important is a change of 0.03 in the value of $\log_{10} A$ or an alteration of ν by 0.16? To answer these questions, the effect of the changes on the geometry of the calculated curves was examined. The temperature values belonging to α=0.3, 0.5 and 0.7 were used for this purpose. $T_{0.5}$ characterizes the position of the calculated curves along the temperature axis, while the $\Delta T = T_{0.7} - T_{0.3}$ difference serves as a measure

of the width of the curves. The obtained values were compared to their counterparts in Evaluation 3 and only small changes were observed, as the last two rows of Table 5 indicate.

When all kinetic parameters were allowed to have different values for the CRR experiments, the evaluation became an ill-defined task. In this case the kinetic parameters of the CRR experiments migrated to meaningless values while the deviations between the measured and the observed data were much lower than the real reliability of the CRR experiments during the whole convergence.

Table 5: Tests on the Difference between the Gasification at Highly Different Reaction Rates and Reaction Temperatures[a,b]

	Parameters allowed to differ for the CRR experiments					
	A	A, E	A, ν	A, n	A, E, ν	A, ν, n
Identifier of the evaluation	i	ii	iii	iv	v	vi
N_{param}	8	9	9	10	11	11
$100\sqrt{\overline{of}} - 100\sqrt{\overline{of_{eval3}}}$	-0.01	-0.01	-0.02	-0.03	-0.02	-0.05
$\overline{log_{10}A_{lin\&mod}} - \overline{log_{10}A_{CRR}}$	0.00	–	-0.02	-0.01	-0.005	-0.03
$E_{lin\&mod} - E_{CRR}$	–	0.3	–	–	0.3	–
$\nu_{lin\&mod} - \nu_{CRR}$	–	0.12	-0.12	–	-0.12	-0.16
$\overline{n_{lin\&mod}} - \overline{n_{CRR}}$	–		–	-0.03	–	-0.03
$\overline{T_{0.5,CRR}} - \overline{T_{0.5,CRR,eval3}}$	-0.3	-0.4	0.0	-0.3	0.0	0.4
$\overline{\Delta T_{CRR}} - \overline{\Delta T_{CRR,eval3}}$	0.3	0.2	-0.3	0.0	0.0	-0.5
$\overline{T_{0.5,lin\&mod}} - \overline{T_{0.5,lin\&mod,eval3}}$	0.0	-0.1	0.0	-0.1	0.0	-0.1
$\overline{\Delta T_{lin\&mod}} - \overline{\Delta T_{lin\&mod,eval3}}$	-0.3	-0.2	-0.3	-0.4	-0.4	-0.3

[a] The arithmetic means are denoted by upper bars. Subscripts *CRR* and *lin&mod* refer to the CRR experiments and to the group of experiments with linear and modulated *T(t)*, respectively. Subscript *eval3* indicates the corresponding results from Evaluation 3, when none of the parameters were allowed to vary by T(t). The dimension of A is s^{-1}. [b] $T_{0.5}$ (°C) and ΔT (°C) are the temperature belonging to α=0.5 and a measure of the peak width of a given $m^{calc}(t)$ function, respectively, as explained in the text.

4. CONCLUSION

(1) The CO_2 gasification of chars was investigated at slow heating programs, under well-defined conditions on samples prepared from Norway spruce and its forest residue. Low sample masses were employed to avoid the self-cooling of the samples due to the high enthalpy change of the reaction. The volatile content of the samples was negligible hence the gasification reaction step could be studied without the disturbance of the devolatilization reactions. The forest residue char was more reactive; the temperatures at the half of the mass loss showed 20 – 34 °C differences between the two chars at 10°C/min heating rates.

(2) Six TGA experiments were carried out for each sample with three different temperature programs in 60 and 100% CO_2, respectively. Strongly different temperature programs were selected to increase the information content available for the modeling: linear, modulated and constant-reaction rate (CRR) temperature programs. The ratio of the highest and lowest peak maxima was around 27 in the set of the experiments used for the evaluation. The temperatures at the half of the mass loss differed by around 120°C between the linear and the CRR experiments. In this way the obtained models described the experiments in a wide range of experimental conditions. This arrangement served to increase the experimental information on which the evaluation was based on. The number of experimental curves per number of determined kinetic parameters varied between 1.5 and 2.4 in the evaluations.

(3) All experiments were measured by 1 and 2 mg initial sample masses. Thermal lags due to self-cooling were observed in the 2 mg experiments at 10°C/min heating rate. Nevertheless, the evaluation of the 2 mg experiments resulted in essentially the same kinetic parameters as the 1 mg experiments.

(4) A relatively simple and widely used reaction kinetic equation described well the experiments. The dependence on the reacted fraction as well as the dependence on the CO_2 concentration were described by power functions (n-order reactions). The evaluations were also carried out with an $f(\alpha)$ function that can mimic the various random pore / random capillary models. These attempts, however, did not result in improved fit.

(5) Nearly identical activation energy values were obtained for the chars made from wood and forest residues (221 and 218 kJ/mol, respectively). Accordingly a common E for the two chars could be assumed without a loss in the fit quality. The assumption of a common reaction order on the CO_2 concentration had only negligible effect on the fit quality: $\sqrt{of}$ increased only by a factor of 1.006. The assumption of common reaction orders on both the CO_2 concentration (ν) and 1-α (n) resulted in a 1.09 times increase in $\sqrt{of}$. In this approximation the reactivity differences between the two chars are expressed only by the preexponential factor.

(6) The question arose: are the kinetic parameters influenced by the roughly 120°C temperature difference between the CRR and the other experiments? Test evaluations were carried out to clarify this aspect. Parts of the kinetic parameters were allowed to be different for the CRR experiments and the rest of the experiments so that a potential difference between the CRR and the other experiments could be manifested in the changes of the corresponding parameters. However, only slight differences were obtained and the higher number of the parameters hardly changed the fit quality.

AUTHOR INFORMATION

Corresponding Author

* To whom correspondence should be addressed. E-mail: varhegyi.gabor@t-online.hu, Tel. +36 1 2461894, Fax: +36 1 4381147.

ACKNOWLEDGMENT

The authors acknowledge the financial support by the Research Council of Norway and a number of industrial partners through the project GasBio ("Gasification for Biofuels"). G.V. is grateful for the support of the Hungarian National Research Fund (OTKA K72710).

NOMENCLATURE

α = reacted fraction (dimensionless)

ν = reaction order with respect of CO_2 concentration

A = pre-exponential factor in eq 2 (s^{-1})

C_{CO_2} = V/V concentration of the ambient CO_2 (dimensionless)

dev = root mean square of the deviations between the observed and calculated values of a DTG curve (μg/s)

E = activation energy (kJ/mol)

f = empirical function (equations 1, 2, and 8) expressing the change of the reactivity as the reactions proceed (dimensionless)

h_k = either the height of an experimental curve (s^{-1}) or 5×10^{-4} s^{-1}, whichever is higher

m = the sample mass normalized by the initial sample mass (dimensionless)

n = reaction order with respect of 1-α (dimensionless)

o.f. = the objective function minimized in the least squares evaluation (dimensionless)

N_{exper} = number of experiments evaluated together by the method of least squares

N_k = number of evaluated data on the kth experimental curve

N_{param} = number of parameters determined in the evaluation of a series of experiments

R = gas constant (8.3143×10^{-3} kJ mol^{-1} K^{-1})

rel.dev = the deviation (*dev*) expressed as per cent of the corresponding peak height

t = time (s)

T = temperature (°C, K)

z = formal parameter in eq 8 (dimensionless)

REFERENCES

1. Wang, L.; Skjevrak, G.; Hustad, J. E.; Grønli, M. G. Effects of sewage sludge and marble sludge addition on slag characteristics during wood waste pellets combustion. *Energy Fuels*, **2011**, *25*, 5775-5785.

2. Brough, P.; Rørstad, P. K.; Breland, T. A.; Trømborg, E., Exploring Norwegian forest owner's intentions to provide harvest residues for bioenergy. *Biomass and Bioenergy* **2013**, doi:10.1016/j.biombioe.2013.04.009.

3. Werkelin, J.; Skrifvars, B.-J.; Zevenhoven, M.; Holmbom, B.; Hupa M. Chemical forms of ash-forming elements in woody biomass fuels. *Fuel* **2010**, *89*, 481-493.

4. Ahmed, I. I.; Gupta, A. K. Kinetics of woodchips char gasification with steam and carbon dioxide. *Appl. Energy*, **2011**, *88*, 1613-1619.

5. Guizani, C.; Escudero Sanz, F.J.; Salvador, S. The gasification reactivity of high-heating-rate chars in single and mixed atmospheres of H_2O and CO_2. Fuel, **2013**, *108*, 812-823.

6. Prins, M. J.; Ptasinski, K. J.; Janssen, F. J. J. G., From coal to biomass gasification: Comparison of thermodynamic efficiency. *Energy* **2007**, *32*, 1248-1259.

7. Abdullah, H.; Wu, H., Biochar as a Fuel: 1. Properties and Grindability of Biochars Produced from the Pyrolysis of Mallee Wood under Slow-Heating Conditions. *Energy Fuels* **2009**, *23*, 4174-4181.

8. De Groot, W. F.; Shafizadeh, F. Kinetics of Douglas fir and cottonwood chars by carbon dioxide. *Fuel* **1984**, *63*, 210-216.

9. Cozzani, V. Reactivity in oxygen and carbon dioxide of char formed in the pyrolysis of refuse-derived fuel. *Ind. Eng. Chem. Res.* **2000**, *39*, 864-872.

10. Ollero, P; Serrera, A.; Arjona, R.; Alcantarilla, S. The CO_2 gasification kinetics of olive residue. *Biomass Bioenergy* **2003**; *24*, 151-161.

11. Gómez-Barea, A.; Ollero, P.; Fernández-Baco, C. Diffusional effects in CO_2 gasification experiments with single biomass char particles. 1. Experimental investigation. *Energy & Fuels* **2006,** *20*, 2202-2210.

12. Di Blasi, C. Combustion and gasification rates of lignocellulosic chars. *Prog. Energy Combust. Sci.* **2009,** *35*, 121-140.

13. Huang, Y.; et al., Effects of metal catalysts on CO_2 gasification reactivity of biomass char. *Biotechnol. Advances*, **2009**, *27*, 568-572.

14. Khalil, R.; Várhegyi, G.; Jäschke, S.; Grønli, M. G.; Hustad, J. CO_2 gasification of biomass chars. A kinetic study. *Energy Fuels* **2009**, *23*, 94-100.

15. Seo, D.K.; Sun Ki Lee, S. K.; Kang, M. W.; Hwang, J.; Yu, T. U. Gasification reactivity of biomass chars with CO_2. *Biomass Bioenergy*, **2010**, *34*, 1946-1953.

16. Mitsuoka, K., Hayashi, S.; Amano, H.; Kayahara, K.; Sasaoaka, E.; Uddin, M. A.; Gasification of woody biomass char with CO_2: The catalytic effects of K and Ca species on char gasification reactivity. Fuel Processing Technology, 2011. *92*, 26-31.

17. Yuan, S.; Chen, X. L.; Li,J.; Wang, F. C. CO_2 gasification kinetics of biomass char derived from high-temperature rapid pyrolysis. *Energy Fuels*, **2011**, *25*, 2314-2321.

18. Vamvuka, D.; Karouki, E.; Sfakiotakis S. Gasification of waste biomass chars by carbon dioxide via thermogravimetry. Part I: Effect of mineral matter. *Fuel* **2011**, *90*, 1120-1127.

19. Vamvuka, D.; Karouki, E.; Sfakiotakis, S.; Salatino, P. Gasification of waste biomass chars by carbon dioxide via thermogravimetry – effect of catalysts. Combust. Sci. Technol. **2012**, *184*, 64-77.

20. Burhenne, L., Damiani, M.; Aicher, T. Effect of feedstock water content and pyrolysis temperature on the structure and reactivity of spruce wood char produced in fixed bed pyrolysis. *Fuel*, **2013**, *107*, 836-847.

21. Kirtania, K.; Joshua, J.; Kassim, M. A.; Bhattacharya, S. Comparison of CO_2 and steam gasification reactivity of algal and woody biomass chars. *Fuel Process. Technol.* **2013**, http://dx.doi.org/10.1016/j.fuproc.2013.02.006.

22. Di Blasi, C.; Buonanno, F.; Branca, C. Reactivities of some biomass chars in air, Carbon **1999**, *37*, 1227-1238.

23. Várhegyi, G.; Mészáros, E.; Antal, M. J., Jr.; Bourke, J.; Jakab, E. Combustion kinetics of corncob charcoal and partially demineralized corncob charcoal in the kinetic regime. *Ind. Eng. Chem. Res.* **2006**, *45*, 4962-4970.

24. Werkelin, J.; Skrifvars, B.-J.; Hupa, M., Ash-forming elements in four Scandinavian wood species. Part 1: Summer harvest. *Biomass Bioenergy* **2005**, *29*, , 451-466.)

25. High resolution thermogravemetric analysis - A new technique for obtaining superior analytical results. TA Instruments report TA-023. Available at: http://www.tainstruments.co.jp/application/pdf/Thermal_Library/Applications_Briefs/TA023.PDF

26. Becidan, M.; Várhegyi, G.; Hustad, J. E.; Skreiberg, Ø. Thermal decomposition of biomass wastes. A kinetic study. *Ind. Eng. Chem. Res.* **2007**, *46*, 2428-2437.

27. Tapasvi, D.; Khalil, R.; Várhegyi, G.; Skreiberg, Ø.; Tran, K.-Q.; Grønli, M.: Kinetic behavior of torrefied biomass in an oxidative environment. *Energy Fuels*, **2013**, *27*, 1050-1060.

28. Várhegyi, G. Aims and methods in non-isothermal reaction kinetics. *J. Anal. Appl. Pyrolysis* **2007**, *79*, 278-288.

29. Várhegyi, G.; Sebestyén, Z.; Czégény, Z.; Lezsovits, F.; Könczöl, S. Combustion kinetics of biomass materials in the kinetic regime. *Energy Fuels*, **2012**, *26*, 1323-1335.

30. Várhegyi, G.; Chen, H.; Godoy, S. Thermal decomposition of wheat, oat, barley and Brassica carinata straws. A kinetic study. *Energy Fuels* **2009**, *23*, 646-652.

31. Várhegyi, G.; Szabó, P.; Mok W. S. L., Antal, M. J., Jr.: Kinetics of the thermal decomposition of cellulose in sealed vessels at elevated pressures. Effects of the presence of water on the reaction mechanism. *J. Anal. Appl. Pyrolysis* **1993**, *26*, 159-174.

32. Bhatia; S. K; Perlmutter, D. D. A random pore model for fluid–solid reactions: I. Isothermal kinetic control. *AIChE J.* **1980**, *26*, 379-386.

33. Gavalas, G. R. A random capillary model with application to char gasification at chemically controlled rates. *AIChE J.* **1980**, *26*, 577-585.

34. Várhegyi, G.; Szabó, P.; Jakab, E.; Till, F.; Richard J-R. Mathematical modeling of char reactivity in Ar-O_2 and CO_2-O_2 mixtures. *Energy Fuels* **1996**, *10*, 1208-1214.

35. Grønli, M.; Antal, M. J., Jr.; Várhegyi, G. A round-robin study of cellulose pyrolysis kinetics by thermogravimetry. *Ind. Eng. Chem. Res.* **1999**, *38*, 2238-2244.